Signatures of Accretion Shocks in Broadband Spectrum of Advective Flows Around Black Holes

Samir Mandal

Centre for Space Physics, Chalantika 43, Garia Station Rd., Kolkata 700084;
space_phys@vsnl.com

Sandip K. Chakrabarti*

S.N. Bose National Centre for Basic Sciences,
JD-Block, Sector III, Salt Lake, Kolkata 700098, India
chakraba@bose.res.in

We compute the effects of the centrifugal pressure supported shock waves on the emitted spectrum from an accretion disk primarily consisting of low angular momentum matter. Electrons are very efficiently accelerated by the accretion shock and acquire power-law distribution. The accelerated particles in turn emit synchrotron radiation in presence of a stochastic magnetic field in equipartition with the gas. Efficient cooling of the electrons by these soft photons reduces its temperature in comparison to the protons. We explore the nature of the broadband spectra by using Comptonization, bremsstrahlung and synchrotron emission. We then show that there could be two crossing points in a broadband spectrum, one near $\sim 10keV$ and the other $\sim 300 - 400$KeV.

Keywords: Black hole physics; accretion; spectral properties; synchrotron radiation; shock waves

1. Introduction

It is more than fifty years since the study of the accretion flows on to gravitating compact objects began. Bondi[1] first showed that spherically symmetric matter would pass through a sonic sphere before falling on a sufficiently compact object. However, the matter has a large radial motion. Close to the black hole, velocity is very high, and thus the density is low. As a result, the flow has a very low radiation efficiency. Discovery of quasars and active galaxies in this decade required that the efficiency be improved. For this, several important steps were taken. First, Shvartsman[2] introduced dissipation due to entangled magnetic field. Shapiro[3−4] computed the degree of dissipation and found that the luminosity is increased by a

*Also at Centre for Space Physics, Chalantika 43, Garia Station Rd., Kolkata 700084

significant amount. However, this was still not sufficient to explain quasar luminosity. Shakura-Sunyaev[5] introduced Keplerian thin disk models of the active galaxies. These are efficient and did indeed explain the 'big blue bump' in UV/EUV region of the spectra of the active galaxies[6]. However, power-law high energy X-rays could not be accounted for by this model. Chang and Ostriker[7] and Kazanas and Elision[8] resorted to introducing accretion shocks where the temperature and density would be enhanced and the radiation efficiency is also increased. The former introduced pre-heating dominated shocks at a very large distance from the black hole, while the latter introduced pair-plasma pressure supported shocks close to the black hole. Chakrabarti[9−10] showed that centrifugal barrier in a low angular momentum accretion flow can produce stable shocks for a wide range of parameter space provided the flow has specific angular momentum everywhere small compared to the Keplerian value. This work was further put to test by Chakrabarti and Wiita[11] and Chakrabarti and Titarchuk[12] who showed that shocks could play a major role in determining the spectrum of the emitted radiation. Particularly important is that, post-shock region which is known as the CENBOL (Centrifugal pressure Supported Boundary Layer) and which is the repository of hot electrons, can easily inverse Comptonize photons from a Keplerian disk located in the pre-shock region and the power-law component of the flow may be formed easily without taking resort to any hypothetical electron cloud originally invoked in the literature[13−17]. Thus, the CENBOL region in between the horizon and the shock as introduced by Chakrabarti and his co-workers behave like a boundary layer where the flow dissipates its gravitational energy. Furthermore, shocks have been found to be oscillating when the cooling is introduced and this is explained to be the cause of the quasi-periodic oscillations in X-rays[18].

However, astrophysical shocks also play a major role in acceleration of particles. It is well known that the high energy cosmic rays are produced by shock acceleration[19−21]. These shocks are transient in nature and still play an important role in shaping the spectrum. Hence, it is likely that the *standing shocks*, through which majority of the accreting matter must *pass* before entering into a black hole, or forming a jet, should be important to energize electrons. This shocks are very stable and remain virtually in place even after non-axisymmetric perturbations[22]. It is thus fitting that we be interested to understand how the energetics of the high energy electrons is affected by these shocks and how the spectrum is affected by the synchrotron radiation produced by these energetic particles.

In Section 2, we present the basic equations and the relevant parameters for the problem. We assume the Paczynski-Wiita[23] potential to describe the space-time around a non-rotating black hole. We introduce a major emitting component, the accretion shocks. In Section 3, we present the relevant heating and cooling processes which are taking place in the accretion flow. In Section 4, we discuss how a broad band spectra may be obtained. In Section 5, we present a typical spectrum and its components. We also give particular emphasis to high energy gamma-ray emissions in hard and soft states. Finally, in Section 6, we present concluding remarks.

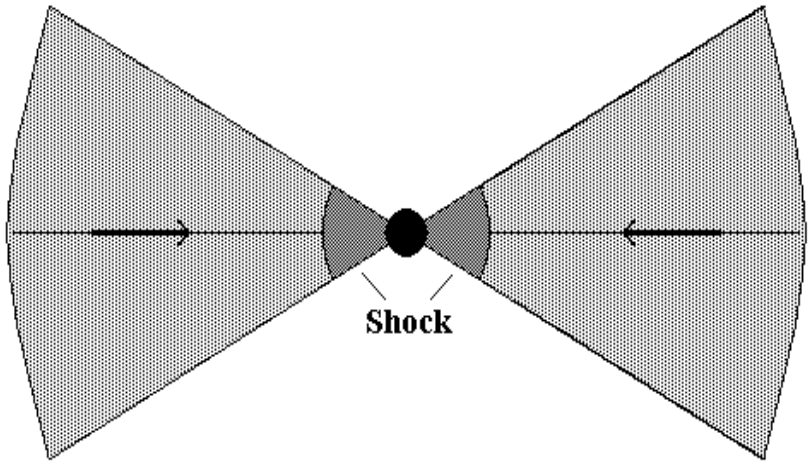

Fig. 1: Cartoon diagram of a quasi-spherical, low-angular momentum accretion around a compact object. Dark shaded region indicates a standing shock formed by centrifugal force.

2. Basic Hydrodynamic Equations

As far as the flow topology is concerned, we assume it to be thin, axi-symmetric, and of conical cross-section. The flow is assumed to be from winds of the companion star as in the case of a stellar black hole, or supermassive black holes. We do not consider the presence of a Keplerian disk, or, if present it is assumed to be very far from the region of consideration. The motivation of our present work is to see what the advective disk emits through bremsstrahlung, Comptonization and synchrotron emission. In a future work we shall incorporate the Keplerian disk as well.

Figure 1 gives a cartoon diagram of the flow geometry we consider in this paper. The low angular momentum flow roughly moves as a freely falling gas in the Paczynski-Wiita[23] potential with the velocity profile:

$$v(x) = (x-1)^{-1/2}, \tag{1}$$

where x is the radial distance in units of the Schwarzschild radius, $r_g = 2GM/c^2$, c is velocity of light, G is the gravitational constant and M is the mass of the central black hole. The electron number density, determined from the mass conservation law assuming pure hydrogen, is given by,

$$n(x) = \frac{\dot{M}}{\Omega m_p x^2 v(x)}, \tag{2}$$

where the geometric factor Ω arises because we are assuming conical flow of solid

angle Ω (instead of 4π valid for a Bondi flow),

$$\Omega = 4\pi cos(\Theta), \tag{3}$$

where Θ is the angle made by the surface of the flow with the vertical axis. $\dot{M}$ is the mass accretion rate and m_p is proton mass. In presence of pure hydrogen, Thomson scattering will be the most dominating scattering process and the corresponding optical depth is given by,

$$\tau(x) = \frac{4\pi}{\Omega}(\frac{\dot{m}}{2})\int_{\infty}^{x} \frac{\sqrt{x-1}}{x^2}dx, \tag{4}$$

where $\dot{m}$ is the mass accretion rate in units of Eddington rate $\dot{M}_{Edd}$

$$\dot{m} = \frac{\dot{M}}{\dot{M}_{Edd}}. \tag{5}$$

We calculate the magnetic field at a given radial distance from the equipartition between the gravitational energy density and the magnetic energy density i. e.,

$$\frac{B^2}{8\pi} = \frac{GM\rho}{(x-1)}. \tag{6}$$

Using (1) and (2), the energy balance equations for protons and electrons can be written as,

$$\frac{dT_p}{dx} + \frac{T_p(3x-4)}{3x(x-1)} + \frac{\Omega m_p}{k\dot{M}}\frac{2}{3}x^2(\Gamma_p - \Lambda_p) = 0, \tag{7a}$$

$$\frac{dT_e}{dx} + \frac{3}{2}(\gamma-1)\frac{T_e(3x-4)}{3x(x-1)} + \frac{\Omega m_p}{k\dot{M}}(\gamma-1)x^2(\Gamma_e - \Lambda_e) = 0, \tag{7b}$$

where, γ is 5/3 for non-relativistic electron temperatures ($T_e \leq m_e c^2/k$) and 4/3 for relativistic electron temperatures ($T_e > m_e c^2/k$). k is the Boltzmann constant. Since protons are much heavier than the electrons, T_p always remains in the non-relativistic domain. Γ and Λ contain contributions from all the heating and cooling processes respectively. Detailed nature of these terms will be discussed below.

It has been shown[9−10] that the shocks in a black hole geometry can typically occur at around $x_s \sim 5-300r_g$ depending on the specific angular momentum λ. We do not explicitly solve for the shock locations in this paper. Thus, instead of using λ as a free parameter as in Chakrabarti[9−10], we use x_s to be the free parameter. In a transonic solution, the shock strength is also computed from the inflow parameters. We use R, the compression ratio, to be a free parameter as well.

3. Heating and Cooling Processes

First of all, we neglect heating due to dissipation as far as the protons are concerned. Protons lose energy through Coulomb interaction Λ_{ep} and inverse bremsstrahlung Λ_{ib}. So,

$$\Lambda_p = \Lambda_{ep} + \Lambda_{ib}. \tag{8}$$

Here, the subscript p represents protons. The effect of Λ_{ib} is generally much smaller than Λ_{ep}. Electron-proton coupling supplies energy to the electrons (from protons) and is given by,

$$\Lambda_{ep} = 1.6 \times 10^{-13} \frac{k\sqrt{m_e} ln\Lambda_0}{m_p} n^2 (T_p - T_e) T_e^{-3/2}, \tag{9}$$

where, $ln\Lambda_0$ is the Coulomb logarithm, m_p and m_e are the rest masses of proton and electron respectively. Electrons are heated through this Coulomb coupling.

$$\Gamma_e = \Lambda_{ep}. \tag{10}$$

Subscript e represents electrons.

Cooling terms for the electrons include bremsstrahlung Λ_b, cyclo-synchrotron Λ_{cs} and Comptonization Λ_{mc} of the soft photons due to cyclo-synchrotron radiation. For the time being we ignore any Keplerian flow on the equatorial plane which could also supply soft photons. The effect of this would be to introduce a bump in the soft X-ray and a power-law component due to Comptonization[12]. The net cooling of the electrons is:

$$\Lambda_e = \Lambda_b + \Lambda_{cs} + \Lambda_{mc}. \tag{11}$$

Explicit expressions for the cooling terms for electrons satisfying Maxwell-Boltzmann distribution are:

$$\Lambda_{ib} = 1.4 \times 10^{-27} n^2 \Big(\frac{m_e}{m_p} T_p\Big)^{1/2} \tag{12a}$$

$$\Lambda_b = 1.4 \times 10^{-27} n^2 T_e^{1/2} (1 + 4.4 \times 10^{-10} T_e) \tag{12b}$$

$$\Lambda_{cs} = \frac{2\pi}{3c^2} k T_e(x) \frac{\nu_a^3}{x}, \tag{12c}$$

where ν_a is the critical frequency at which the self-absorbed synchrotron radiation spectrum is peaked and it can be determined from the relation,

$$\nu_a = \frac{3}{2} \nu_0 \theta_e^2 x_m \tag{13}$$

where,

$$\nu_0 = 2.8 \times 10^6 B, \tag{14a}$$

$$\theta_e = \frac{kT_e}{m_e c^2}. \tag{14b}$$

Procedure to determination of x_m is discussed below.

When the injected electrons obey a power-law distribution, the expressions given above will change. For instance, the cooling term due to cyclo-synchrotron photons would be given by,

$$\Lambda_{cs} = \mathcal{A}\mathcal{G} B^{(p+1)/2} (\nu_{max}^{(3-p)/2} - \nu_{min}^{(3-p)/2}) \tag{15}$$

where,

$$\mathcal{A} = \frac{(3\pi)^{1/2} K e^3}{m_e c^2 (1+p)(3-p)} (\frac{2\pi m_e^3 c^5}{3e})^{(1-p)/2}, \tag{16a}$$

$$\mathcal{G} = \frac{\Gamma(p/4+19/12)\Gamma(p/4-1/12)\Gamma(p/4+5/4)}{\Gamma(p/4+7/4)}. \tag{16b}$$

and K is the normalization constant of power-law electron distribution,

$$n(\mathcal{E}) = K\mathcal{E}^{-p}, \tag{17}$$

which is obtained using the constraint that the electron number is conserved during shock acceleration. The Comptonization is computed by using this cooling term augmented by the enhancement factor $\mathcal{F}$:

$$\Lambda_{mc} = \Lambda_{cs}\mathcal{F}. \tag{18}$$

For Comptonization of the thermal seed photons by thermal electrons, $\mathcal{F}$ is given by[17],

$$\mathcal{F} = \eta_1 \Big\{ 1 - \Big(\frac{x_a}{3\theta_e} \Big)^{\eta_2} \Big\}, \tag{19}$$

where,

$$\eta_1 = \frac{P(A-1)}{(1-PA)}, \tag{20a}$$

$$P = 1 - exp(-\tau_{es}), \tag{20b}$$

is the probability that an escaping photon is scattered, while,

$$A = 1 + 4\theta_e + 16\theta_e^2, \tag{21}$$

is the mean amplification factor in the energy of a scattered photon when the scattering electrons have a Maxwellian velocity distribution of temperature θ_e, $\eta_2 = 1 - \frac{lnP}{lnA}$ and $x_a = h\nu_a/m_e^2c^2$. For Comptonization of the non-thermal seed photons (such as generated by the power-law electrons) by thermal electrons, the amplification factor can be written as[24],

$$\mathcal{F} = \eta_1 [1 - (\frac{s}{\phi_s}) \frac{x_{max}^{\phi_s} - x_a^{\phi_s}}{3\theta_e(\phi-1)(x_{max}^s - x_a^s}], \tag{22}$$

where,

$$x_{max} = \frac{h\nu_{max}}{m_e c^2}, \tag{23a}$$

$$s = \frac{5-p}{2}, \tag{23b}$$

$$\phi_s = \phi + \frac{3-p}{2}, \tag{23c}$$

and

$$\phi = \eta_2 - 1. \tag{23d}$$

The amplification factor[25] for the seed photons comptonized by the electrons obeying power-law distribution can be written as,

$$\mathcal{F} = \frac{4}{3}\sigma_T R_c K \frac{(\mathcal{E}_{max}^{3-p} - \mathcal{E}_{min}^{3-p})}{(3-p)}, \tag{24}$$

where R_c is the size of the Comptonized region. $\mathcal{E}_{max}$ and $\mathcal{E}_{min}$ are maximum and minimum energy of the power-law electrons respectively and σ_T is the Thomson scattering cross-section.

In presence of both thermal and non-thermal electrons x_m has to be calculated by equating combined thermal and non-thermal emission from the CENBOL with the appropriate source functions[26] We ignore the effects of power-law electrons on the emission of bremsstrahlung radiation since this radiation is very weak. The spectral index is computed by standard procedure[17,26] .

4. Solution Procedure

For a given set of initial parameters, we fix the outer boundary at a large distance (say, $10^6 r_g$) and supply matter (both electrons and protons) with the same temperature (say, $T_p = T_e = 10^6 K$). Our result is insensitive to this outer radius as long as it is beyond $\sim 10^3 r_g$ or so. Radial dependence of velocity and density is chosen to be those of the freely falling matter (1). We then use Runge-Kutta method to integrate (7a-b) simultaneously to obtain the electron and proton temperatures as a function of radial distance. After we obtained the density and the temperature at any point, we compute the radiation emitted by the flow through bremsstrahlung and synchrotron radiation. The degree of interception of these low energy photons are computed from the corresponding optical depth these intercepted low energy photons are then inverse Comptonized by the hot electrons in the flow. The rest are allowed to escape from the flow directly to the observer. We followed the procedures presented in Chakrabarti & Titarchuk[12] while computing the Comptonized spectrum except that our soft-photon source is distributed throughout the flow in the form of bremsstrahlung and synchrotron emission. At the end, we add all the contributions to get the net photon emissions from the flow. The geometry of the flow is chosen to be conical. The angle Θ subtended by the flow surface with the z-axis is chosen to be a parameter.

The shock of compression ratio R causes the formation of power-law electrons of slope[19−20]:

$$p = (R+2)/(R-1). \tag{25a}$$

This power-law electrons produce a power-law synchrotron emission with index q given by[21]

$$q = (1-p)/2. \tag{25b}$$

The power-law electrons have energy minimum at

$$\mathcal{E}_{min} = m_e c^2 \Gamma_{min} \tag{26a}$$

and have energy maximum at

$$\mathcal{E}_{max} = m_e c^2 \Gamma_{max} \tag{26b}$$

obtained self-consistently by conserving the number of power-law electrons and by computing the number of scatterings that the electrons undergo inside the disk before they escape. This yields,

$$\Gamma_{max} = \Gamma_{min}[1 + \frac{4}{3}\frac{R-1}{R}\frac{1}{x_s^{1/2}}]^{x_s^{1/2}}. \tag{27}$$

The minimum value of the Lorentz factor Γ_{min} is obtained from the temperature of the injected electrons. This temperature is obtained self-consistently through our integration procedure. Earlier it has been shown[27] that not all the matter actually passes through the shock. Only when the flow passes close to the equatorial plane actually passes through a shock. Furthermore, this fraction is time dependent for oscillating shocks[28]. Thus, in the absence of a fully time dependent solution, we assume the percentage of electrons ζ acquiring a power-law energy distribution to be a free parameter.

We thus have a complete recipe for generating a broad band spectra as a function of the following parameters: Θ, x_s, R, ζ and $\dot{m}$. The relevant ranges are: $0 < \Theta < 90$ $5 < x_s < 300$, $0 < R < 4$, $0 < \zeta < 1$, $10^{-5} \gtrsim \dot{m} \lesssim 3$. The upper limit of R is obtained[29] for a gas of polytropic index 5/3:

$$R_{strong} = \frac{\gamma + 1}{\gamma - 1}. \tag{28}$$

In the next Section, we discuss the nature of a typical spectrum obtained for a black hole of mass $10 M_\odot$. Our procedure is equally valid for massive and supermassive black holes in Active Galactic Nuclei, and this will be discussed elsewhere.

5. Results and Interpretations

5.1. *A Typical Broadband Spectrum*

Figure 2 shows the variation of the electron (dotted) and proton (solid) temperatures (T_e and T_p respectively) when $\dot{m} = 0.1$, $R = 3.9$, $\Theta = 77^o$, $\zeta = 0.4$ and $x_s = 80$ as a function of the radial distance x (measured in units of the Schwarzschild radius r_g). Both the axis are in logarithmic scale. It is clear that since Coulomb coupling is not very strong, the heating of the electrons is not very efficient. Thus, they start becoming cooler closer to the black hole when the number density becomes higher. Higher number density increases the cooling of the electrons for $x \lesssim 300$. Very close to the black hole, especially after the shock at $x = x_s = 80$, the splitting is dramatic and electrons become cooler more rapidly.

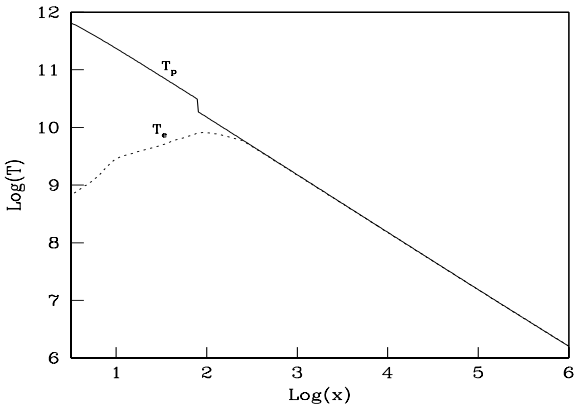

Fig. 2: Variation of the electron (dotted) and proton (solid) temperatures (T_e and T_p respectively) when $\dot{m} = 0.1$, $R = 3.9$, $\Theta = 77^o$, $\zeta = 0.4$ and $x_s = 80$ as a function of the radial distance x. As flow comes closer to the black hole, the temperatures separate due to fast cooling of the electrons due to synchrotron radiation.

In Figure 3, we present a typical spectrum with all the contributions from the accretion flow. The parameters chosen are the same as above. Here, different curves are marked with a number.

The curve marked '1' is the synchrotron emission from the pre-shock part of the accretion flow. The curve marked '2' is the Comptonized spectrum of pre-shock synchrotron photons due to thermal electrons. The curve marked '3' gives the bremsstrahlung emission from the pre-shock region and curve marked '4' is the corresponding Comptonized spectrum. The curve marked '5' indicates the synchrotron spectrum from the post-shock region. Comptonized spectra of the synchrotron radiation from the post-shock accretion flow due to thermal and non-thermal electrons are indicated in curves marked '6' and '7' respectively. The curve marked '8' and '9' represents respectively the bremsstrahlung emission and it's Comptonization from the post-shock flow. The curve marked '10' is the total broad-band spectra from the pre-shock and the post-shock regions. ν_a indicates the synchrotron self-absorption frequency.

It is clear that the power-law electrons, which are the hall-mark of the shock in accretion can leave its signature on the emitted spectrum. The curve '6' is soft and thermal component, while the curve '7' is hard and is generally from the non-thermal power-law component emitted by the power-law electrons.

When the shock-location is varied, the following changes are expected: when the shock is located very close to the black hole, the hot pre-shock flow is the dominant source of Comptonized photons while when the shock is very far away, the post-shock region (CENBOL) also contributes, but as a whole, the contribution is much lower as the outer flow is cooler. When the compression ratio is varied, the optical depth in the post-shock region is changed. For a weak shock, the jump in density $\rho^+ = R\rho_-$, where + and − denote the post and pre-shock values respectively, at

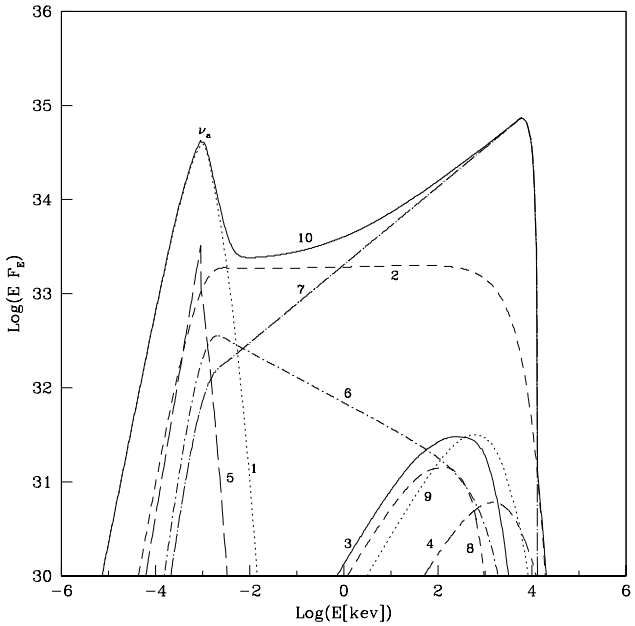

Fig. 3: A typical broad-band spectrum with all the contributions from the accretion flow is shown for the same parameter as in Fig. 2 (see text for details).

the shock is not so high. In this case, the power law electrons are not energetic enough to leave its signature in the spectrum. When the accretion rate increased, it is expected to increase the density of the flow and it becomes difficult to cool the matter by the soft photons of the synchrotron radiation. The Comptonized spectrum becomes harder. At lower accretion rate, it is easy to cool the flow and the spectrum becomes softer. When the percentage of power-law electrons, namely, ζ is increased the spectrum becomes harder at high energy.

5.2. *Spectra in Soft and Hard States*

We now discuss the basic changes in the flow properties which must occur if the spectral state is to switch from hard to soft state (in soft-X-ray region) and vice versa. In Fig. 4, we present the photon spectra in the hard and the soft states. The hard state was created with $\dot{m} = 1.0$, $R = 4$, $x_s = 180$, $\Theta = 80$ and $\zeta = 0.01$. In the soft state, the accretion rate $\dot{m} = 0.1$, $x_s = 50$ and $\zeta = 0.7$ was chosen. Other parameters were kept fixed. Here too, we did not consider the presence of a Keplerian disk, which can also supply soft photons, as we are interested only in the behaviour of an advective flow.

In the soft state, the spectral slope is high and the energy spectral index α_t ($F(E) \propto E^{-\alpha_t}$) from the photons from thermal electrons is found to be $\alpha_t = 1.47$

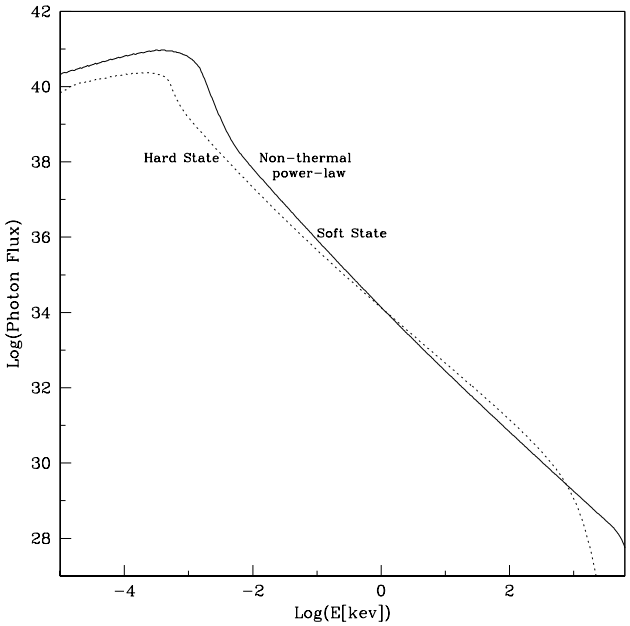

Fig. 4: State transitions occurring in a black hole candidate when the accretion rate and the shock location is varied. The thermal bump in the hard state causes two intersections to form one at a few keV and the other at a few hundred keV (see text for details).

which that for the not-thermal electrons is $\alpha_{nt} = 0.53$. In the hard state $\alpha_t = 0.45$ and $\alpha_{nt} = 1.35$. Because of the thermal bump at around 100keV, the two spectra intersect at two energies, one at lower energy ($\sim 4-10$keV) and the other at a high energy $\sim 300-400$keV. Normally, the intersection at the lower energy is a pivotal point[12]. In Fig. 5 we zoom the high energy region of the spectrum and show the nature of the each components. The thermal component in the hard state is from the thermal electrons in the pre-shock and the post-shock flow. The non-thermal power-law component in the hard state is coming from the power-law electrons in the post-shock region. The non-thermal component in the soft-state is from non-thermal electrons.

If one compares with observation one notices that the black hole candidates Cyg X-1[30−31] GROJ1719-24 and GROJ4022+32 all show the similar characteristics as presented in Fig. 5 (see, Ling & Wheaton[32] and references therein). We therefore believe successful reproduction of the salient features in our solution shows that the non-thermal emission, at least in these class of black holes, is probably coming from the accretion flow itself.

In Fig. 6, we have presented the variation of the spectral indices of the thermal component and the non-thermal components as function of the sub-Keplerian rate

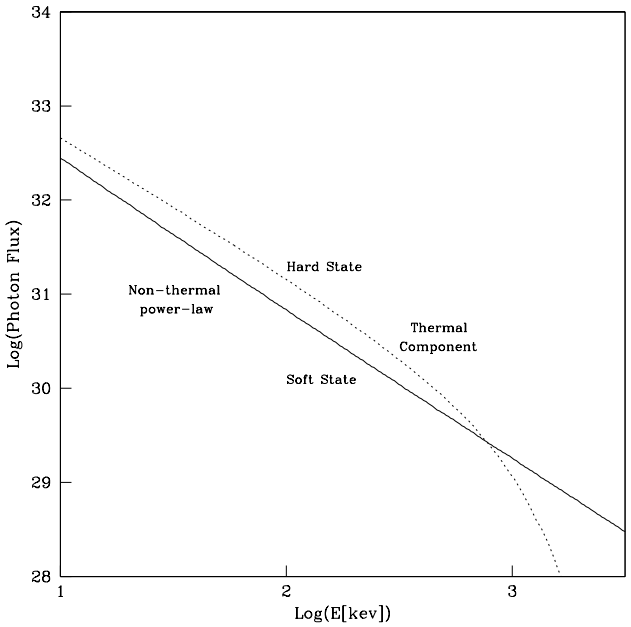

Fig. 5: The spectra in soft and hard states are shown only at high energy region. The thermal bump is due to thermal electrons from the post-shock region while the non-thermal power-law components are due to non-thermal electrons generated by the shock-acceleration.

$\dot{m}$. The other parameters are, $R = 3.9,\ x_s = 10.0,\ \Theta = 77$, and $\zeta = 0.7$. Generally speaking, both the spectral indices decrease initially with the accretion rate but after about an Eddington rate, where the optical depth itself started getting larger than unity, the spectra start becoming softer as expected.

6. Concluding Remarks

In this paper, we have explored the way a shock in an accretion flow may be identified by observing the spectrum. We have used the shock location and its strength as free parameters (at the expense of the specific angular momentum and viscosity parameters) although we have used reasonable values discussed in earlier analytical studies. We considered the soft photons due to bremsstrahlung and synchrotron radiation as the seed photons for the Comptonization. We also included the shock acceleration of the electrons and their effect on the emitted spectrum. We have incorporated the splitting of temperature of the electrons and protons due to radiative processes.

Our conclusion is that there are several ways a shock may be distinguished in the spectrum. At a strong shock, the power-law electrons are produced with a very high γ_{max} and that produces a power-law feature in the spectrum. These power-law features are seen in both the hard and the soft components in the same manner

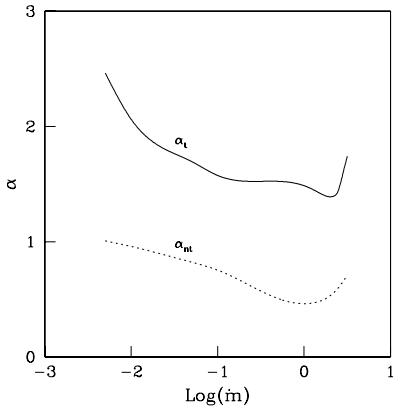

Fig. 6: Variation of the spectral slopes of the thermal and the non-thermal components α_t and α_{nt} respectively as a function of the dimensionless accretion rate.

as observed in the galactic black hole candidates such as Cyg X-1, GROJ1719-24 and GROJ4022+32. We find that since the shocks are inbuilt in the advective disk solutions, and electrons can easily produce high energy radiation first through shock acceleration and then through synchrotron emission, one need not invoke extra source of high energy photons as are usually done in the literature[33−34]. The outflow that is derived from a CENBOL itself can have shocks in jets which in turn may also emit power-law emissions and contribute to the total spectra. We shall explore this aspect of the problem in near future.

In Chakrabarti & Titarchuk[12] soft photons due to a Keplerian disk was responsible to cool down the post-shock region. In the present paper, we deviate from that paper in the sense that we assume that the Keplerian disk is either located very far away, or non-existent. The soft photons are locally generated due to thermal and magnetic bremsstrahlung processes. In presence of a Keplerian disk, the soft X-ray bump will be produced at around a few KeV, while for shocks the bump is located in UV. Thus, it is possible that these two distinct bumps can be distinguished through observation. This work will also be presented elsewhere.

There has been mush discussions about the so-called advection dominated accretion flows or ADAF (see, Esin et al.[35] and references therein) which also claims to produce quasi-spherical accretion accretion as the transonic flows described in Chakrabarti[10]. However, ADAFs or any of its modifications do not have any shocks as in our transonic solution and therefore they need to invoke external sources of non-thermal electrons. Thus our solutions require lesser parameters that the class models based on ADAF.

This work is partly supported by a RESPOND project funded by Indian Space Research Organization (ISRO).

References

1. H. Bondi, *Mon. Not. Roy. Astron. Soc.*, **112**, 195 (1952)
2. V. F. Shvartsman, *Sov. Astron. A. J.*, **15**, 377 (1971)
3. S. L. Shapiro, *Astrophys. J.*, **180**, 531 (1973)
4. S. L. Shapiro, *Astrophys. J.*, **183**, 69 (1973)
5. N. I. Shakura and R. Sunyaev,*Astron. Astrophys.*, **24**, 337 (1973)
6. M. Malkan and W. Sergent, *Astrophys. J.*, **254**, 22 (1982)
7. K. M. Chang and J. P. Ostriker, *Astrophys. J.* **288**, 428 (1985)
8. D. Kazanas and D. C. Ellison, *Astrophys. J.*, **304**, 178 (1986)
9. S. K. Chakrabarti, *Mon. Not. Roy. Astron. Soc.*, **283**, 325 (1996)
10. S.K. Chakrabarti, *Theory of Transonic Astrophysical Flows* (World Scientifc Publishers: Singapore) (1990)
11. S. K. Chakrabarti and P. J. Wiita, *Astrophys. J.*, **387**, L21 (1992)
12. S. K. Chakrabarti and L. G. Titarchuk, *Astrophys. J.*, **455** 623 (1995)
13. R. I. Sunyaev and L. G. Titarchuk, *Astron. & Astrophys.*, **86** 121 (1980)
14. R. I. Sunyaev and L. G. Titarchuk, *Astron. & Astrophys.*, **143** 374 (1985)
15. A. A. Zdziarski, *Astrophys. J.*, **289** 514 (1985)
16. B. E. Stern, et al. *Astrophys. J.*, **449**, L113 (1995)
17. Titarchuk, L.G. and Lyubarskij, Y., *Astrophys. J.*, 450, 876, (1995)
18. S. K. Chakrabarti and S. G. Manickam, *Astrophys. J.*, **531**, L41 (2000)
19. A. R. Bell, *Mon. Not. Roy. Astron. Soc.*, **182**, 147 (1978)
20. A. R. Bell, *Mon. Not. Roy. Astron. Soc.*, **182**, 443 (1978)
21. M. S. Longair, *High Energy Astrophysics*, (Cambridge Univ. Press: UK) (1981)
22. D. Molteni, G. Tóth and O. A. Kuznetsov *Astrophys. J.*, **516**, 411 (1999)
23. B. Paczynski and P. J. Wiita, *Astron. Astrophys.* **88** 23 (1980)
24. Dermer, C.D,. Liang, E.P. and Canfield, E., *Astrophys. J.*, 369, 410 (1991)
25. Rybicki, G. B. & Lightman, A.P., *Radiative Processes in Astrophysics*, (Wiley Interscience: New York) (1979)
26. Mandal, S. & Chakrabarti, S. K. , *Astron. & Astrophys.* (submitted)
27. D. Molteni, G. Lanzafame and S. K. Chakrabarti, *Astrophys. J.*, **425**, 161 (1994)
28. D. Molteni, G. Sponholz and S. K. Chakrabarti *Astrophys. J.*, **457**, 805 (1996)
29. L. Landau and E. M. Lifshitz, *Fluid Mechanics* (Pergamon Press: New York) (1959)
30. M. L. McConnell et al. *Astrophys. J.* **572** 984 (2002)
31. K. Pottschmidt et al. *Astron. Astrophys.* **411** 383 (2003)
32. Ling, J. C. and Wheaton, W. A., *Chinese J. Astron. Astrophys.* (in press)
33. D. Lin & E. P. Liang *Astron. Astrophys.* **341** 954 (1999)
34. G. Wardzinski and A.A. Zdziarski, **Mon. Not. Roy. Astron. Soc. 325**, 963 (2001)
35. A. A. Esin, R. Narayan, W. Cui, J. E. Grove and S.-N. Zhang, *Astrophys. J.* **505** 854 (1998)